

Purple sweet potato delphinidin-3-rutin represses glioma proliferation by inducing miR-20b-5p/Atg7-dependent cytosstatic autophagy

Meng Wang,^{1,3,5} Ke Liu,^{1,4,5} Huimin Bu,¹ Hao Cong,¹ Guokai Dong,¹ Nana Xu,¹ Changgen Li,¹ Yunyun Zhao,¹ Fei Jiang,¹ Yongjing Zhang,¹ Bo Yuan,¹ Rongpeng Li,¹ and Jihong Jiang^{1,2}

¹Key Laboratory of Biotechnology for Medicinal Plants of Jiangsu Province, School of Life Sciences, Jiangsu Normal University, Xuzhou, Jiangsu 221116, People's Republic of China; ²College of Pharmacy, Zhejiang Chinese Medical University, Hangzhou, Zhejiang 310053, People's Republic of China; ³Public Experimental Research Center, Xuzhou Medical University, Xuzhou, Jiangsu 221004, People's Republic of China; ⁴Xuzhou Administration for Market Regulation, Xuzhou, Jiangsu 221000, People's Republic of China

Glioma is the most common primary malignant intracranial tumor. Owing to highly aggressive invasiveness and metastatic properties, the prognosis of this disease remains poor even with surgery, radiotherapy, and chemotherapy. Rutin is a glycoside natural flavonoid that modulates microglia inflammatory profile and improves anti-glioma activity. Here, a glycoside flavonoid was extracted and named purple sweet potato delphinidin-3-rutin (PSPD3R). In an experiment using the subcutaneous xenograft model of human glioblastoma (GBM) and alamar blue assay, we found that PSPD3R suppressed the glioma proliferation both *in vitro* and *in vivo*. Flow cytometry assay and transmission electron microscopy observation revealed that PSPD3R stimulated glioma cell autophagy and apoptosis. High-throughput microRNA (miRNA) sequencing showed that PSPD3R substantially affected the miRNA expression of U251 cells. Acridine orange staining and immunoblotting indicated that PSPD3R regulated autophagy via Akt/Creb/miR-20b-5p in glioma cells. Luciferase reporter assays showed that autophagy-related gene 7 (Atg7) mRNA was the target gene of miR-20b-5p. The downregulation of miR-20b-5p inhibited glioma proliferation *in vivo*. In summary, PSPD3R regulated autophagy in glioma via the Akt/Creb/miR-20b-5p/Atg7 axis. This work unraveled the molecular mechanism of PSPD3R-induced autophagy in glioma and revealed its potential as a therapeutic agent for glioma treatment.

including natural products such as flavonoids, terpenoids, cannabin, and so on.⁴

Natural products for glioma therapy mainly consist of polyphenolic compounds that have been widely recognized and could effectively pass through the blood-brain barrier.^{5,6} *In vitro* and *in vivo* studies on glioma models revealed that these compounds exhibit anti-tumor effects by modulating angiogenesis, migration, invasion, proliferation, apoptosis, and chemoresistance signaling pathway.⁷ For example, resveratrol could cross the blood-brain barrier and influence the central nervous system, thus suppressing oxidative stress and neuroinflammation and inducing the apoptosis of glioma cells to inhibit their proliferation.⁸ Curcumin exerts an anti-tumor effect by inducing excessive autophagy in A172 human glioblastoma (GBM) cells⁹; pine bark polyphenolic extract could attenuate amyloid- β and -tau misfolding in the model system of Alzheimer's disease neuropathology.¹⁰ To date, research on glioma-related compounds has only focused at the phenotypic level, and their molecular mechanisms are rarely reported. Therefore, the theoretical basis for combining immunotherapy with chemotherapy or targeted therapy in glioma is lacking, and natural products have not been clinically applied. Understanding the glioma-regulating mechanism of natural products from the molecular biology point of view could aid in discovering diagnostic biomarkers and specific therapeutic targets and expanding new alternative therapies.¹¹

INTRODUCTION

Glioma is the most common primary intracranial malignant tumor, with extraordinarily high mortality and mean survival of less than 14 months.¹ Its current treatment is the traditional surgical resection combined with fractionated radiotherapy and adjuvant chemotherapy with temozolomide.² Owing to its rapid and infiltrative growth, complete surgical removal is usually not possible. Glioma cells are prone to develop resistance to chemotherapy and radiotherapy; hence, the prognosis remains poor.³ Therefore, the classical treatments must be urgently extended to alternative therapy,

Received 5 January 2022; accepted 22 July 2022;
<https://doi.org/10.1016/j.omto.2022.07.007>.

⁵These authors contributed equally

Correspondence: Rongpeng Li, Key Laboratory of Biotechnology for Medicinal Plants of Jiangsu Province, School of Life Sciences, Jiangsu Normal University, Xuzhou, Jiangsu 221116, People's Republic of China.

E-mail: lirongpeng@jsnu.edu.cn

Correspondence: Jihong Jiang, Key Laboratory of Biotechnology for Medicinal Plants of Jiangsu Province, School of Life Sciences, Jiangsu Normal University, Xuzhou, Jiangsu 221116, People's Republic of China.

E-mail: jhjiang@jsnu.edu.cn



Flavonoids,¹² a polyphenol natural product widely existing in nature, have an antioxidant effect for the treatment of cardiovascular and cerebrovascular diseases, tumors, and inflammation. It has been reported that part of these nature products has no substantial cytotoxicity¹³ and can pass through the blood-brain barrier to ameliorate neurodegenerative diseases.¹⁴ Rutin, a flavonoid glycoside, is present in Chinese medicinal materials, such as *Sophora flavescens*,¹⁵ citrus sinensis peel,¹⁶ and grape wastes.¹⁷ It has been reported that rutin can regulate microglial inflammation and inhibit glioma growth,¹⁸ especially in recurrent cases.¹⁹ Since *Ipomoea batatas Lam*²⁰ has rich nutritional components including anthocyanidins, polysaccharides, plant proteins, vitamins, mineral elements, and rutin, we tried to extract these compounds from medicinal purple sweet potato "Ningzishu No. 4." In previous work, we found that anthocyanin extract from purple sweet potato exacerbates mitophagy to ameliorate pyroptosis in *Klebsiella pneumoniae* infection.²¹ Therefore, we speculated that rutin extracted from purple sweet potato also had an effect of treating glioma.

In this study, a flavonoid glycoside was extracted and named purple sweet potato delphinidin-3-rutin (PSPD3R). PSPD3R was found to inhibit the proliferation of glioma cells and induce their excessive autophagy and apoptosis by regulating microRNAs (miRNAs) *in vitro* and *in vivo*. Further study on the underlying molecular mechanism confirmed that PSPD3R inhibited the phosphorylation of protein kinase B (PKB/AKT) pathways and the dephosphorylation of cyclic adenosine monophosphate (cAMP) response element-binding protein (Creb), downregulated miR-20b-5p, and increased autophagy-related gene 7 (Atg7) expression and LC3-II conversion, all of which eventually led to the excessive autophagy and apoptosis of glioma cells. These findings provide a theoretical basis for the subsequent research and clinical application of PSPD3R.

RESULTS

PSPD3R inhibited glioma cell growth *in vitro* and *in vivo*

First, alamar blue assay was used to test and compare the growth of two human gliomas cells (U251 and A172) with that of several normal control cells (BV2, MHS, MLE-12, human umbilical vein endothelial cells [HUVCEs], and rat astrocyte [AST] cells) following PSPD3R treatment to investigate the anti-cancer effect of PSPD3R on glioma cells. The results showed that PSPD3R exhibited a growth-inhibitory effect on glioma cells but was nontoxic to normal cells. Treatment of 100 μ M PSPD3R caused a massive glioma cell death and left virtually no survivors but almost had no effect on normal cells (Figure 1A). PSPD3R remarkably inhibited the cell viability of gliomas cells in a dose- and time-dependent manner, and treatment with 100 μ M PSPD3R almost suppressed the growth of gliomas cells within 48 h (Figure 1B). Alamar blue assay was also used to screen the 50% lethal dose (LD50) of drug concentrations *in vitro*. The results showed that the PSPD3R-treated glioma cells achieved the LD50 in 50 μ M after 24 h (revised Figure 1B, red arrow). Therefore, 50 μ M was selected as the final concentration in cell culture medium and 24 h as the appropriate treatment time for the following experiments. Clono-

genic survival and EdU proliferation assays were employed to further verify the inhibition effect of PSPD3R on the proliferation of glioma cells. The number of cell clones in PSPD3R-treated U251 and A172 cells was substantially reduced compared with that in the control group, indicating that the proliferation ability of glioma cells was significantly inhibited by PSPD3R (Figure 1C). This finding was further confirmed by the EdU proliferation assay, which revealed a significant reduction in the number of EdU-incorporating live cells among the PSPD3R-treated U251 and A172 cells (Figure 1D).

The establishment of orthotopic xenograft tumors was attempted in the beginning of this study. However, some mice died within 10 days after being inoculated with glioma cells in brain, probably due to intracranial pressure change, resulting in missed data. Thus, the subcutaneous xenogeneic model of Professor Mu and colleagues²² was adopted. This model was also used by Professor Bu and colleagues²³ in their study of lung cancer treatment, implying that the conclusion obtained using this model was credible. According to the results of the present experiments, the subcutaneous xenogeneic model was relatively stable (Figure S1). Therefore, an implanted subcutaneous GBM was established by injecting U251 and A172 cells into Balb/c nude mice, which were then treated with 1 (low dose) or 5 (high dose) mg/kg PSPD3R every 2 days²⁴ to validate whether the *in vitro* anti-tumor effect of PSPD3R is also evident *in vivo* (Figure 2A). The xenografts in the PSPD3R-treated mice grew more slowly than those in the placebo-treated control mice. Meanwhile, the anti-tumor effect of PSPD3R at low doses was weaker than that at high doses (Figure 2A). From a macroscopic view, the tumor size was reduced in the PSPD3R-treated mice compared with that in the control group (Figure 2B). Consistently, the tumor weight of PSPD3R-treated mice was significantly lower than that of the control mice (Figure 2C). In general, a high-dose PSPD3R treatment is more efficient in inhibiting tumor than a low-dose treatment. The xenografts were further stained for Ki67, a marker widely used in assessing the proliferative fraction in cancers, to clarify the role of PSPD3R in proliferation inhibition. The xenografts of PSPD3R-treated mice showed less Ki67 staining than those of the control mice (Figures 2D and S2A). These findings collectively revealed that PSPD3R inhibited the growth of GBM *in vitro* and *in vivo*.

PSPD3R stimulated glioma cell autophagy and led to apoptosis

Autophagy is a double-edged sword for cancer cells that either favors their survival or induces their death under certain stress.²⁵ This process has been recently reported as a potential therapy for malignant glioma.²⁶ In this work, PSPD3R was proposed to inhibit glioma cell growth by inducing autophagy. Apoptosis, necroptosis, and pyroptosis are major cell-death modalities. Flow cytometry assay was used to explore which type of glioma cell death is mediated by PSPD3R. The results showed that the number of apoptotic cells increased after treatment with PSPD3R, indicating that this metabolite induced the apoptosis of glioma cells (Figures 3A and S2B). After the glioma cells were treated with the combination of autophagy inhibitor 3-methyladenine (3-MA)

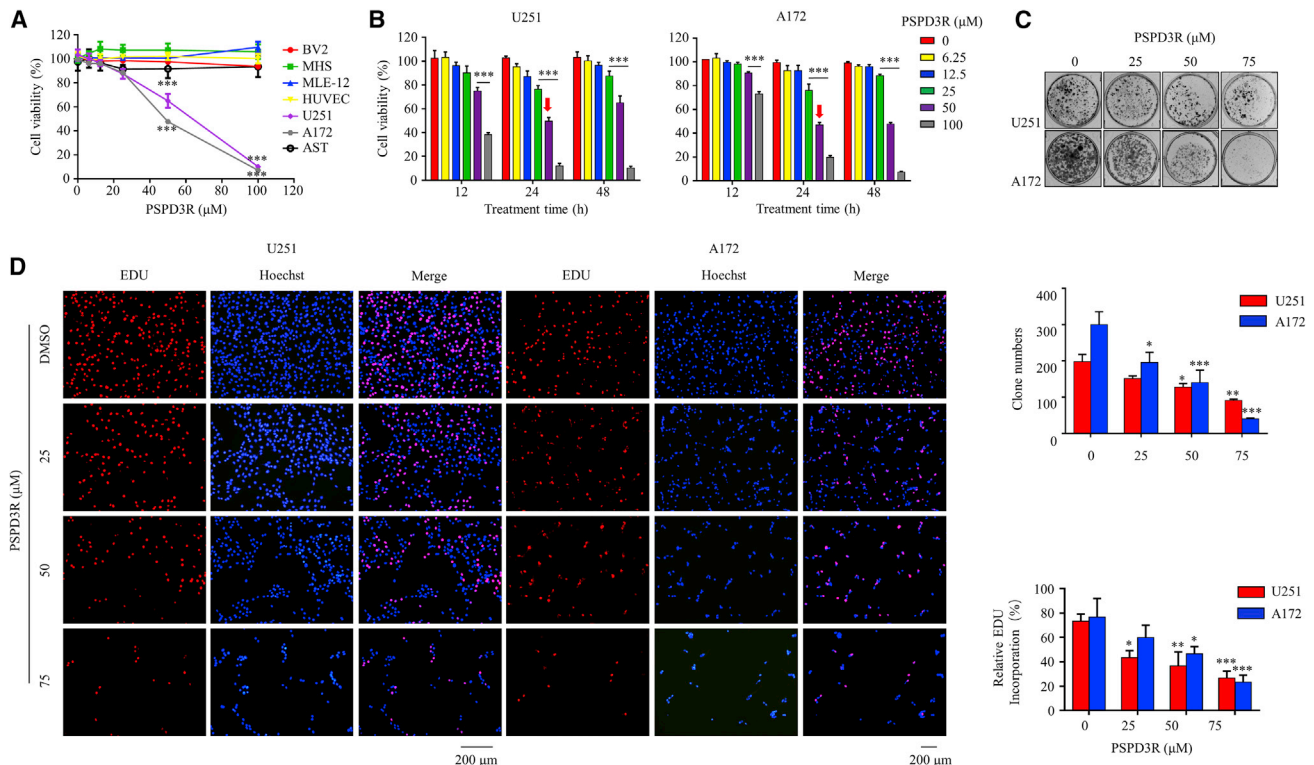


Figure 1. PSPD3R had no toxicity to normal cells but remarkably inhibited the proliferation of gliomas cells in a dose- and time-dependent manner

(A) U251, A172, BV2, MHS, MLE-12, HUVEC, and rat AST cells were incubated in the presence of PSPD3R at different concentrations (0, 6.25, 12.5, 25, 50, or 100 μM) for 48 h, respectively. Cell viability was assessed by alamar blue assay at a wavelength of 530 nm. (B) Anti-cancer activity of PSPD3R. U251 and A172 cells were respectively treated with different concentrations of PSPD3R (0, 6.25, 12.5, 25, 50, or 100 μM) for 12, 24, or 48 h, and cell viability was measured by alamar blue assay. (C) U251 and A172 cells were cultured in the indicated concentrations of PSPD3R for 14 days. The cells were stained with Giemsa stain, and cell clone number was counted. (D) U251 and A172 cells were incubated in the presence of PSPD3R in the indicated concentrations for 24 h. Representative images were provided as indicated; scale bar, 200 μm . Proliferating glioma cells were labeled with EdU fluorescent dye (red), while blue fluorescence indicates DAPI (blue). Cell viability was assessed by EdU incorporation assays. Data are presented as mean \pm SD from three independent experiments. t test for two experimental group comparisons; * $p < 0.05$; ** $p < 0.01$; *** $p < 0.001$.

and PSPD3R, the number of apoptotic cells decreased compared with that in the group treated with PSPD3R alone (Figures 3A and S2B). These data suggested that autophagy might be associated with the death of the treated glioma cells. The ultra-structures of autophagy in glioma cells were then observed by transmission electron microscopy to further confirm whether PSPD3R stimulates autophagy. The results showed that the number of autophagosomes was higher in the PSPD3R-treated glioma cells (U251 and A172) than in the control glioma cells (Figures 3B and S2C), indicating that PSPD3R inhibited glioma cell growth by inducing autophagy.

The formation of acidic vesicular organelles (AVOs) is an indicator of an autophagic process.²⁷ Thus, acridine orange (AO) was used to stain the PSPD3R-treated glioma cells to further study the autophagy induced by PSPD3R. Similar with the results of flow cytometry assay, cytoplasmic AVO formation was quickly observed in the PSPD3R-treated cells compared with that in the control cells and 3-MA/PSPD3R-combined-treated cells (Figures 3C and S2D). This

finding further revealed that PSPD3R induced autophagy in glioma cells.

Immunoblotting assay was used to determine LC3-II conversion after the glioma cells were combined treated with 3-MA and PSPD3R (Figure 3D). PSPD3R induced the accumulation of LC3-II in glioma cells, but the combination treatment of PSPD3R with 3-MA inhibited the accumulation of LC3-II in the treated glioma cells. Alamar blue assay was then applied to verify the viability of the glioma cells after being treated with 3-MA and PSPD3R (Figure 3E), and the results were coincident with the immunoblotting. In summary, PSPD3R induced glioma cell apoptosis via autophagy.

PSPD3R significantly affected the miRNA expression of U251 glioma cells

miRNAs are associated with human tumorigenesis by regulating the expression of oncogenes or tumor-suppressor genes.²⁸ Owing to the relatively high cost of miRNA microarray analysis of miRNAs, which is commonly used to predict underlying molecular mechanism, precise

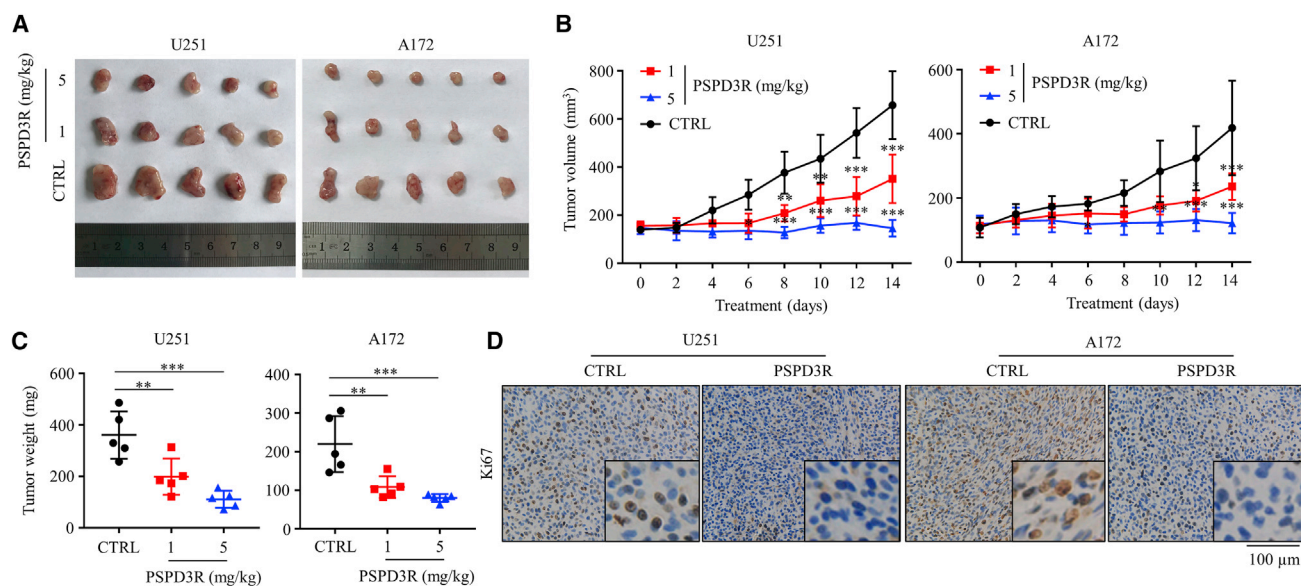


Figure 2. PSPD3R inhibited glioma cell growth *in vivo*

(A–C) 1×10^7 of U251 or A172 cells per mouse were subcutaneously inoculated in the back of Balb/C mice. 1 or 5 mg/kg of PSPD3R was administered by intraperitoneal injection every 2 days. Mice were sacrificed on day 14, and tumors were excised, photographed, measured, and weighted. (D) Ki67 expression in tumor xenografts was examined by immunohistochemical (IHC) staining. Representative images were provided as indicated; scale bar, 100 μ m. Data are presented as mean \pm SD from three independent experiments. t test for two experimental group comparisons; ** $p < 0.01$; *** $p < 0.001$.

molecular experiments must be conducted to confirm the subsequent proof. Therefore, only a representative cell line, U251, was selected for the prediction of properties. High-throughput miRNA sequencing analysis was performed on control versus PSPD3R-treated U251 cells to investigate the effects of PSPD3R on the miRNA expression of glioma cells. Among the 76 miRNAs detected with altered expression levels (Figures 4A and 4B), 72 genes were upregulated, and 4 genes were downregulated. Quantitative real-time polymerase chain reaction (PCR) analysis was performed to validate the high-throughput sequencing data both in U251 and A172 cells. Four downregulated genes and the two most significantly changed genes were chosen and verified to be related to autophagy. In particular, miR-20b-5p showed the highest change both in U251 and A172 cells. In summary, the quantitative real-time PCR data were in accordance with the results of high-throughput sequencing analysis in U251 cells (Figure 4C).

PSPD3R regulated autophagy in glioma cells via miR-20b-5p

Given that PSPD3R induces autophagy in glioma cells and regulates miR-20b-5p expression, it could control autophagy in glioma cells via miR-20b-5p. Transmission electron microscopy was performed to examine the ultra-structures of cell autophagy to investigate whether miR-20b-5p regulates this process. As shown in the representative images of autophagosomes, the number of glioma cells (U251 and A172) transfected with miR-20b-5p inhibitor (20b-5p-in) was higher than that of glioma cells with nonspecific inhibitor (NS-in) (Figure 5A). This finding directly proved that miR-20b-5p inhibited autophagy in glioma cells.

Various approaches were applied to verify the functionality of miR-20b-5p in PSPD3R-treated glioma cells. First, AO staining assay was performed to detect the formation of AVO in cells. Cytoplasmic AVO formation was quickly observed in PSPD3R and nonspecific mimic (NS-m)-treated cells compared with the other groups (Figure 5B).

Second, the conversion of endogenous LC3 puncta and LC3-I to LC3-II (lipidated LC3-I) was analyzed by confocal microscopy observation to investigate the formation of autophagosome membranes in the PSPD3R- and miR-20b-5p-mimic-treated glioma cells. LC3 puncta accumulation was found increased in the PSPD3R- and NS-m-treated cells compared with that in the other groups (Figure 6A).

Finally, immunoblotting assay was conducted to test LC3-II conversion in PSPD3R- and miR-20b-5p-mimic-treated glioma cells. LC3-II conversion was significantly increased in the PSPD3R- and NS-m-treated cells (Figure 6B).

All three experiments indicated that PSPD3R induced glioma cell autophagy; however, the treatment with miR-20b-5p mimic inhibited autophagy in the PSPD3R-treated glioma cells.

PSPD3R induces autophagy in glioma cells through the Akt/Creb signaling pathway

Akt is extensively involved in the regulation of various functions, such as cell survival, proliferation, migration, metabolism, and

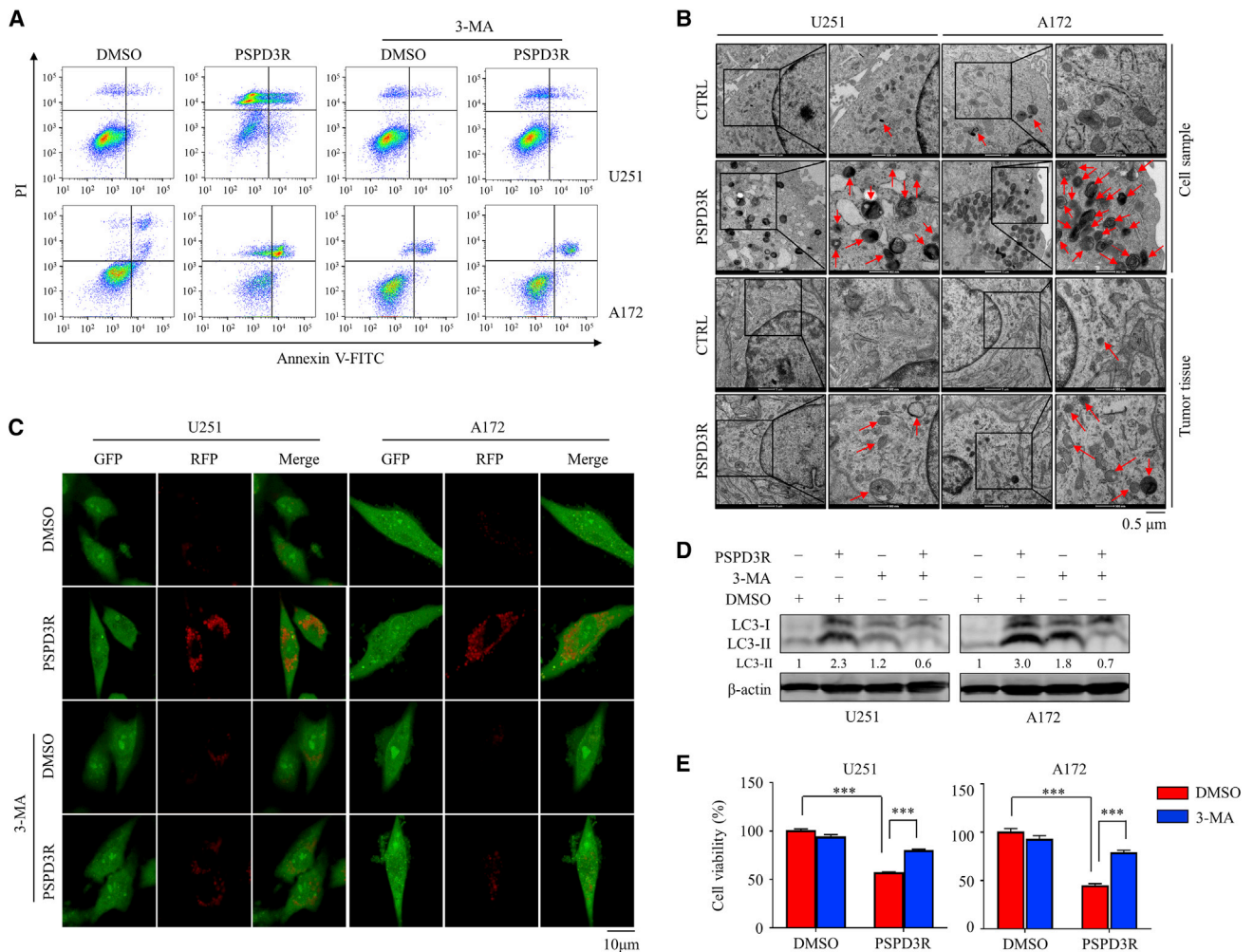


Figure 3. PSPD3R inhibited glioma cell growth by inducing autophagy, but the addition of 3-MA reversed the effect of PSPD3R on glioma cells

(A) U251 and A172 cells were treated with 3-MA in the presence or absence of PSPD3R (50 μ M) for 24 h, then the apoptosis was measured by flow cytometry assay. (B) The autophagy ultra-structure of glioma cells or xenografts was observed by transmission electron microscope. Red arrows, autophagosomes. Scale bar, 0.5 μ m. (C) U251 and A172 cells were treated with 3-MA in the presence or absence of PSPD3R (50 μ M) for 24 h, then cells stained with acridine orange. Autophagosome formation of glioma cells were observed by confocal microscope. Orange puncta were acidic vesicular organelles (AVOs). Scale bar, 10 μ m. (D) LC3 expression level was measured by immunoblotting. (E) Cell viability measured by alamar blue assay of glioma cells treated as in (A). Data are presented as mean \pm SD from three independent experiments. One-way ANOVA (Tukey's post hoc); *** p < 0.001.

angiogenesis.²⁹ Akt is also a central node of many signaling pathways, among which the inhibition of Akt phosphorylation suppresses cell proliferation, one of the pathways of anti-cancer effect.³⁰ Drugs can inhibit the proliferation of cancer cells by inducing autophagy.³¹ Considering our previous study on autophagy (Figure 3), we believed that the autophagy signaling pathway regulated by Akt also plays an important role in inhibiting the proliferation of glioma cells. The pathway in this study would be supplemental to the Akt anti-cancer signaling pathway, and several pathways work together to inhibit the proliferation of cancer cells.

miR-20b-5p was found to be downregulated after PSPD3R treatment; however, the signal pathway that changed its expression in

the PSPD3R-treated glioma cells remains unclear. miR-20b-5p was previously thought to be relevant to the VEGF/Akt/PI3K pathway;³² whether it is regulated by PSPD3R via the Akt pathway remains unknown. Thus, further confirmatory experiments are warranted.

Immunoblotting assay was first used to validate if miR-20b-5p is regulated by PSPD3R via the Akt pathway. The results showed that PSPD3R repressed Akt phosphorylation and significantly increased LC3-II conversion in U251 and A172 cells (Figure 7A). CA-Akt plasmid (used for constitutive expression of active Akt) was transiently transfected into glioma cells to constitutively activate Akt. As a result, PSPD3R-induced Akt/Creb inhibition and LC3-II

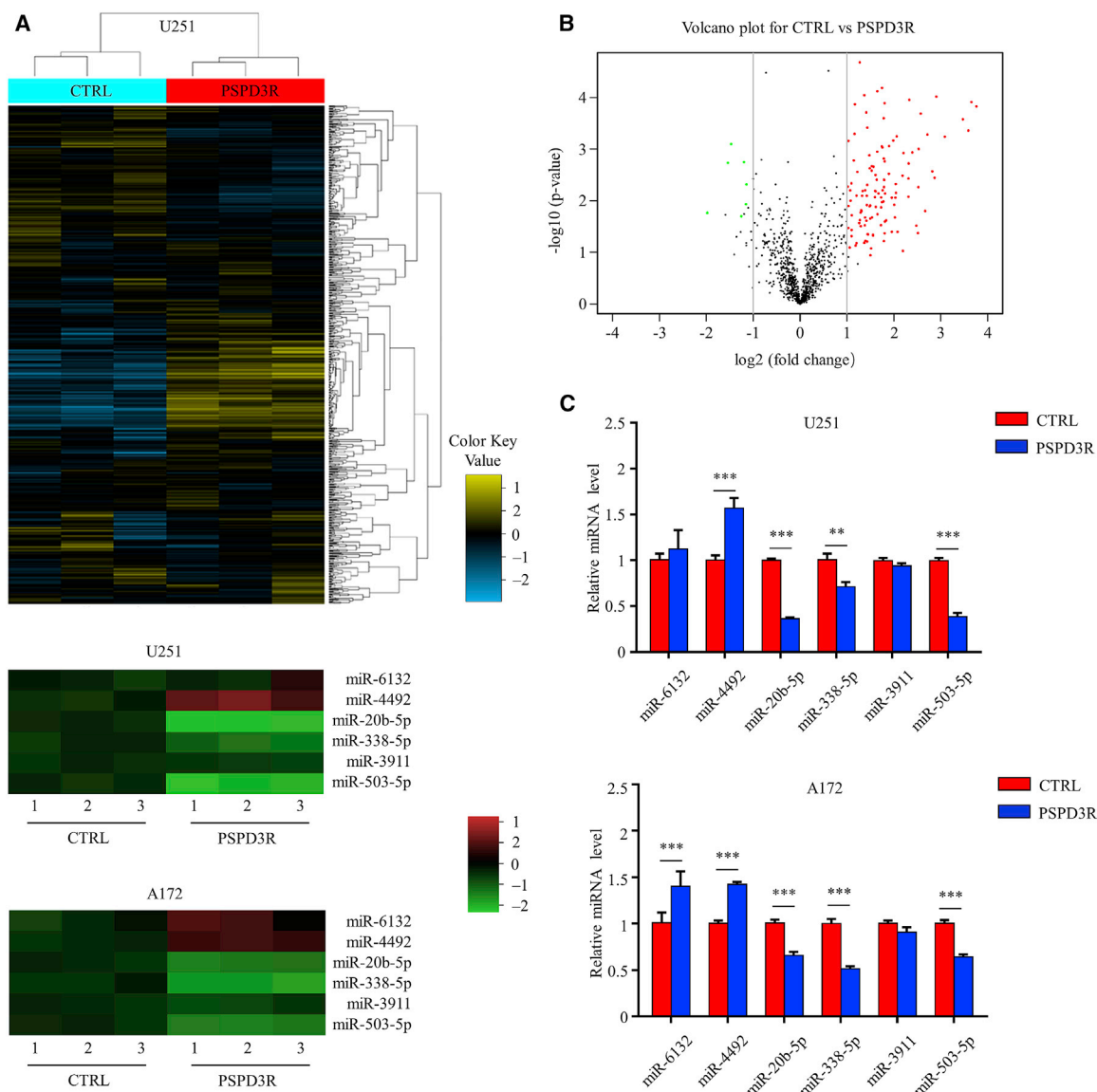


Figure 4. PSPD3R significantly affected the miRNA expression of glioma cells U251

(A) Heatmap of miRNAs in PSPD3R-treated U251 cells by high-throughput sequencing. (B) Volcano plot of miRNA expression profile of PSPD3R-treated U251 cells by miRNA microarray analysis. Red, upregulated genes; green, downregulated genes. (C) The miRNAs levels of U251 and A172 cells were measured by quantitative real-time PCR after treatment with PSPD3R for 24 h. Data are presented as mean \pm SD from three independent experiments. t test for two experimental group comparisons; **p < 0.01; ***p < 0.001.

conversion were recovered (Figure 7B). This finding indicated that PSPD3R affected glioma cells through the Akt pathway.

Although no evidence suggests its relationship to miR-20b-5p, Creb is highly expressed in various malignant tumors and thus is considered a proto-oncogene and transcriptional factor.³³ Hence, miR-20b-5p might be regulated by the transcriptional factor Creb in glioma cells. Additional experiments were needed to further validate this hypothesis. First, immunoblotting assay was used to validate whether

PSPD3R regulates Creb, and the results confirmed that this metabolite repressed Creb phosphorylation (Figure 7A). Furthermore, after the overexpressed Creb plasmid was transiently transfected into glioma cells, the PSPD3R-induced LC3-II conversion was recovered (Figure 7C). Creb short hairpin RNA (shRNA) plasmids (sh-Creb) were also transiently transfected into glioma cells to inhibit Creb expression. This finding revealed that LC3-II conversion was upregulated (Figure 7D), indicating that Creb directly regulated autophagy in glioma cells.

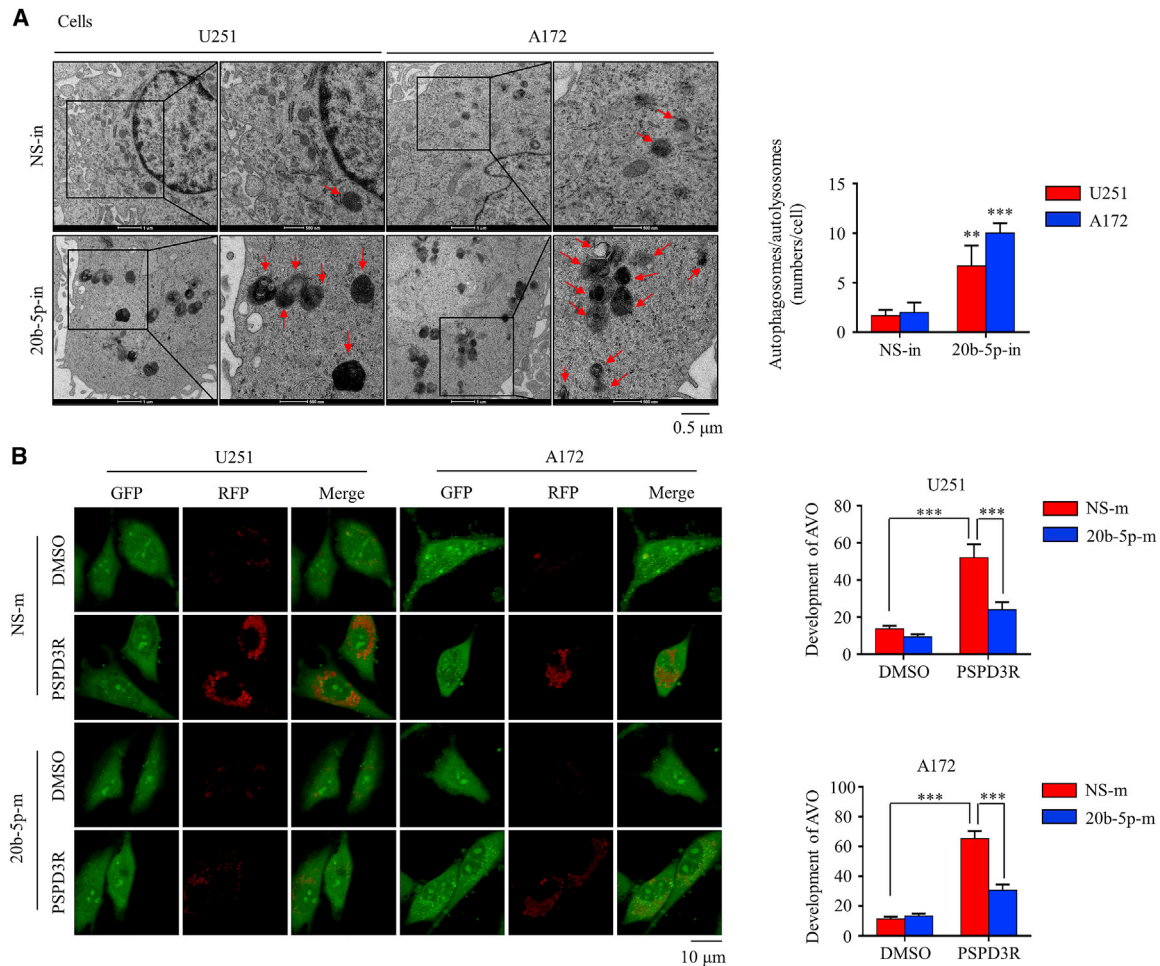


Figure 5. miR-20b-5p inhibitor promoted autophagy in glioma cells, while overexpression of miR-20b-5p inhibited autophagy in PSPD3R-treated glioma cells

(A) U251 and A172 cells were transfected with miR-20b-5p inhibitor (20b-5p-in), then the autophagy ultra-structure of glioma cells was observed by transmission electron microscope. Red arrows, autophagosomes. Scale bar, 0.5 μ m. (B) U251 and A172 cells were transfected with miR-20b-5p mimic (20b-5p-m) or nonspecific control-mimic (NS-m), then cells were incubated with DMSO or PSPD3R (50 μ M) for 24 h. After cells were stained with acridine orange, autophagosome formation of cells was observed under a confocal microscope. Orang puncta were AVOs. Scale bar, 10 μ m. Data are present as mean \pm SD from three independent experiments. One-way ANOVA for multiple comparisons, or t test for two experimental group comparisons; ** $p < 0.01$; *** $p < 0.001$.

AO staining assay was also used to identify if PSPD3R induces autophagy in glioma cells through Creb. The overexpressed Creb plasmid was first transiently transfected into glioma cells, which were then stained with AO. Cytoplasmic AVO formation was quickly observed in the PSPD3R- and vector-treated cells compared with the other groups (Figures 7E and S2E), thus confirming that PSPD3R induced autophagy in glioma cells through Creb.

Quantitative real-time PCR assay was then applied to detect whether Creb alters the expression of miR-20b-5p. sh-Creb plasmids were transiently transfected into glioma cells to inhibit Creb expression. The result showed that miR-20b-5p expression was suppressed in sh-Creb-transfected groups, implying that miR-20b-5p was regulated by Creb (Figure 7F).

All these results provided further evidence that PSPD3R induced autophagy in glioma cells through the Akt/Creb signaling pathway.

PSPD3R promotes autophagy by regulating miR-20b-5p/Atg7 pathway in glioma cells

miRNAs regulate gene expression and eventually affect the expression of their target gene(s). miRanda (Database: <http://www.microrna.org>) was used to predict miRNA target sites and revealed that Atg7 mRNA was the target gene of miR-20b-5p. Thus, PSPD3R increased the Atg7 expression of glioma cells possibly by regulating miR-20b-5p.

Quantitative real-time PCR assay was then applied to detect whether PSPD3R-treated cells alter the expression of miR-20b-5p and Atg7 mRNA in U251 and A172 cells at different time points. Within 4 h,

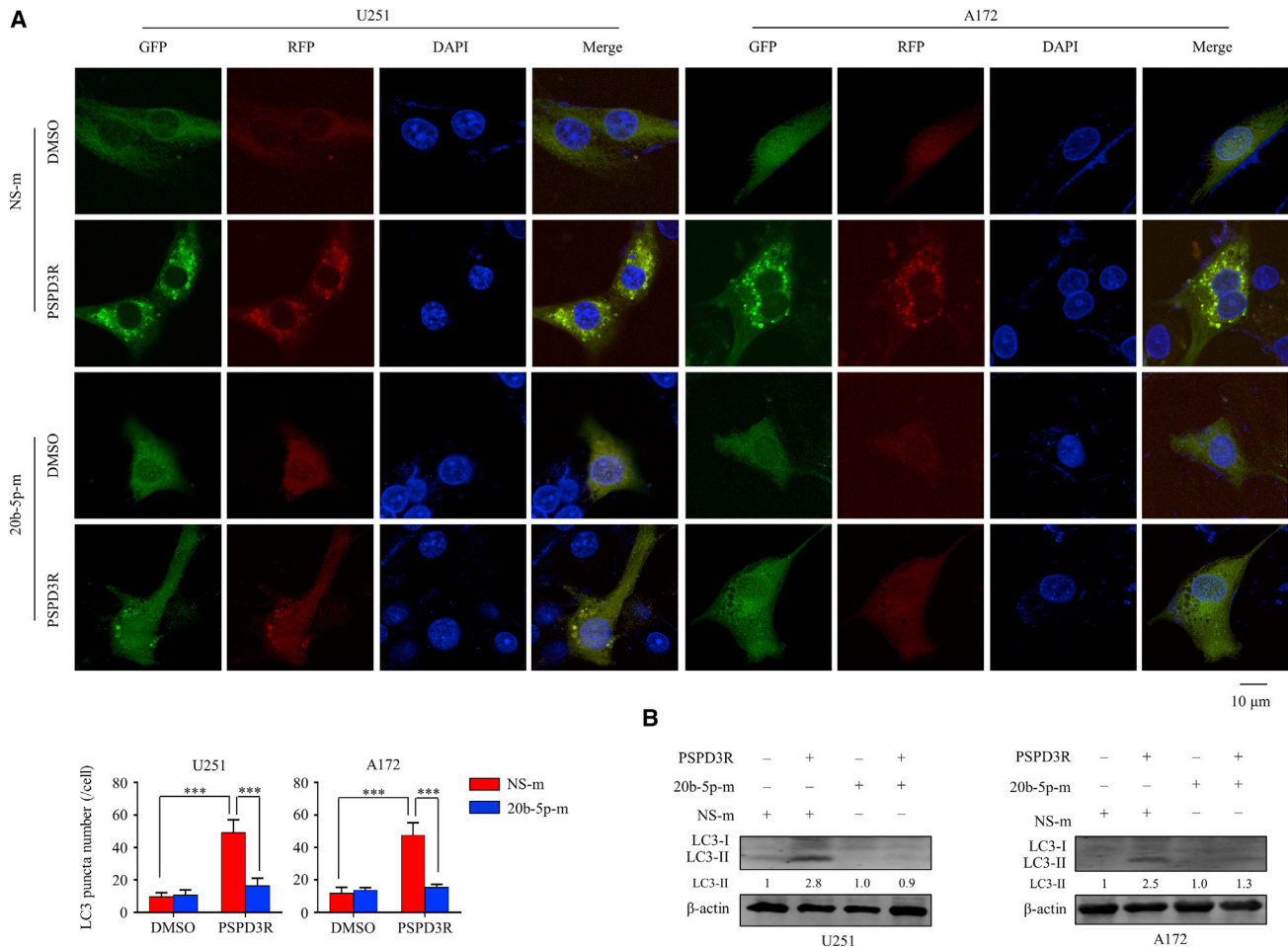


Figure 6. PSPD3R induced glioma cell autophagy, but overexpression of miR-20b-5p reversed the effect of PSPD3R on glioma cells

(A) U251 and A172 cells were cotransfected with GFP-RFP-LC3 plasmid and 20b-5p-m or NS-m for 24 h, then cells were incubated with DMSO or PSPD3R (50 μM) for 24 h. LC3 puncta were detected by confocal microscope. Scale bar, 10 μm. (B) U251 and A172 cells were transfected with 20b-5p-m or NS-m, then cells were incubated with DMSO or PSPD3R (50 μM) for 24 h. LC3 expression was measured by immunoblotting of glioma cells. Cells lysates were collected and then performed for immunoblotting of LC3 lipidation. Data are presented as mean ± SD from three independent experiments. one-way ANOVA for multiple comparisons; ***p < 0.001.

the miR-20b-5p levels were significantly decreased, whereas the Atg7 mRNA levels were significantly increased, in PSPD3R-treated glioma cells (Figure 8A). This result revealed that PSPD3R regulated the expression levels of miR-20b-5p and Atg7 mRNA and that miR-20b-5p had a negative relationship with Atg7 mRNA. Moreover, the mRNA expression of Atg7 was downregulated by miR-20b-5p mimic in U251 and A172 cells (Figure 8B), implying that miR-20b-5p can regulate Atg7 mRNA.

Luciferase assays were used to ensure whether Atg7 mRNA is the direct target of miR-20b-5p. The 3' UTR region of Atg7 was cloned to generate psiCHECK2-Atg7-3' UTR plasmid, and the bind sites between miR-20b-5p were mutated to generate psiCHECK2-Atg7-3'-UTR-mutant (Mut) plasmid (Figure 8C). The results showed that miR-20b-5p significantly decreased the luciferase activity of

psiCHECK2-Atg7-3' UTR-plasmid-transfected cells and had limited effects on the luciferase activity of psiCHECK2-Atg7-3' UTR-Mut-transfected cells (Figure 8D). Therefore, Atg7 mRNA was the direct target gene of miR-20a-5p, and the target site was in the 3' UTR region of Atg7 mRNA.

The suppressive effect of PSPD3R on glioma cells was validated *in vivo*. First, U251 and A172 cells were transfected with lentiviral miR-20b-5p inhibition construct (LV-20b-5p-in) or control LV vector (LV-C). The cells transfected with LV constructs were selected by puromycin and were subcutaneously inoculated in mice. The xenografts in LV-20b-5p-in-transfected mice grew more slowly than those in LV-C-transfected mice (Figure 8E). From a macroscopic view, the tumor size was smaller in the LV-20b-5p-in-transfected mice than in the LV-C-transfected group (Figure 8F). Consistently, the tumor

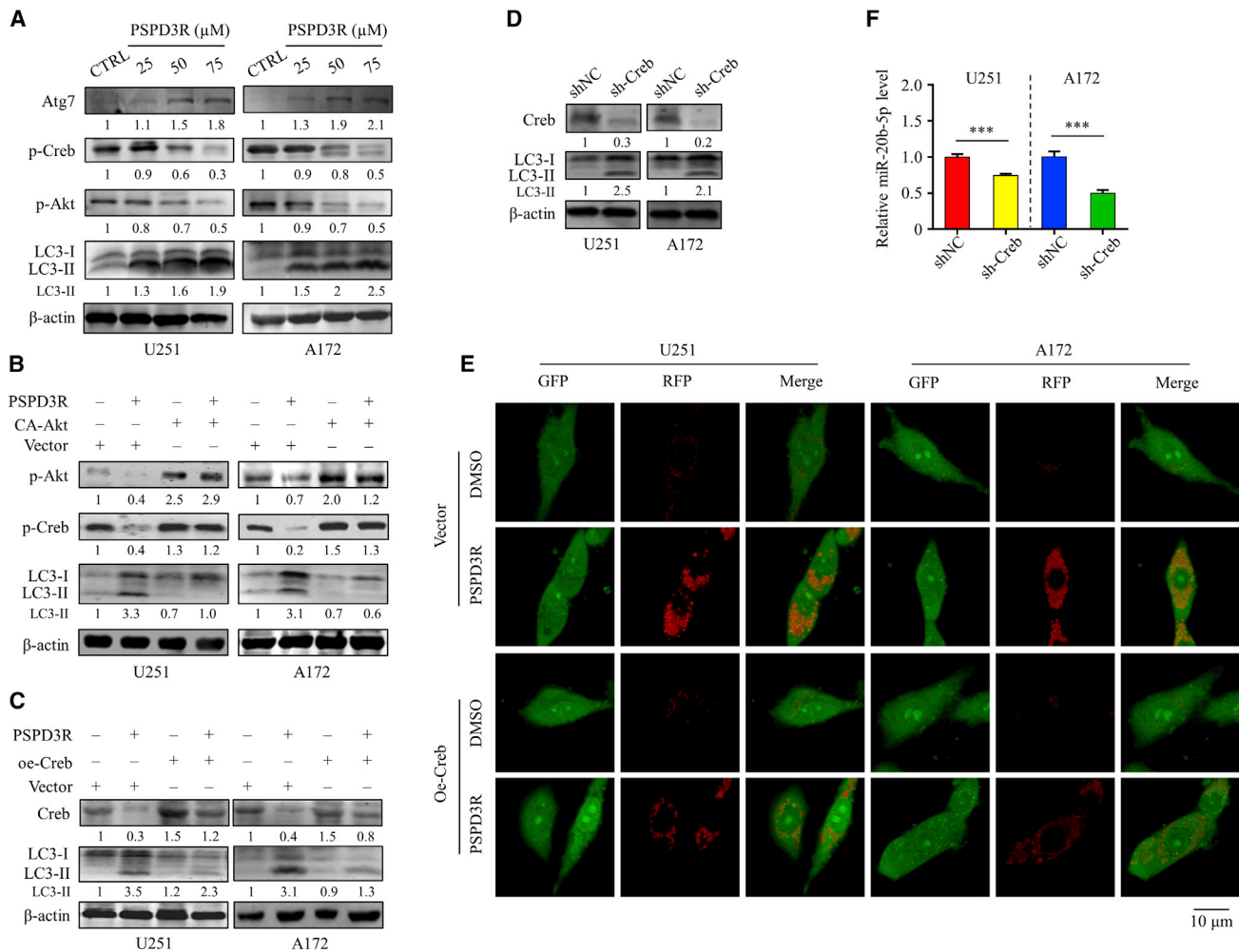


Figure 7. PSPD3R induces autophagy in glioma cells through the Akt/Creb signaling pathway

(A) U251 and A172 cells were treated with the indicated concentrations of PSPD3R for 24 h. Atg7, phosphorylation of Creb and Akt, and LC3 expression were measured by immunoblotting. (B) U251 and A172 cells were transfected with a constitutively active Akt plasmid (CA-Akt) for 24 h and were then treated with 50 μM PSPD3R for another 24 h. Cell lysates were collected and performed for immunoblotting of Akt phosphorylation, Creb phosphorylation, and LC3 lipidation. (C) U251 and A172 cells were transfected with overexpression-Creb plasmid in the presence or absence of PSPD3R (50 μM) for 24 h, and then cell lysates were collected and performed for immunoblotting of Creb and LC3 lipidation. (D) U251 and A172 cells were transfected with Creb shRNA plasmids (sh-Creb), and then cell lysates were collected and performed for immunoblotting of Creb and LC3 lipidation. (E) U251 and A172 cells were transfected with overexpression-Creb plasmid in the presence or absence of PSPD3R (50 μM) for 24 h, and then cells stained with acridine orange. Autophagosome formation of glioma cells were observed by confocal microscope. Scale bar, 10 μm. (F) U251 and A172 cells were transfected with sh-Creb plasmid or shNC, then the expression of Atg7 mRNA was measured by quantitative real-time PCR. Data are presented as mean ± SD from three independent experiments. t test for two experimental groups comparisons; ***p < 0.001.

weight of the LV-20b-5p-in-transfected mice was significantly lower than that of the LV-C-transfected mice (Figure 8G). These data showed that downregulating miR-20b-5p could inhibit the proliferation of glioma cells *in vivo*.

Transmission electron microscopy was used to examine the xenografts from glioma-bearing mice to confirm whether miR-20b-5p regulates autophagy *in vivo*. As shown in the images, the autophagosomes were more abundant in the xenografts of the LV-20b-5p-in-transfected mice than in the xenografts of the LV-C-transfected

mice (Figure 8H). This finding confirmed that the downregulated miR-20b-5p inhibited autophagy *in vivo*.

DISCUSSION

In this study, PSPD3R was found to promote glioma autophagy to apoptosis. The related molecular mechanisms were analyzed in detail for the first time (Figure 8I). *In vitro*, PSPD3R inhibited glioma cell proliferation and promoted apoptosis (Figure 1). This metabolite also suppressed glioma xenograft growth *in vivo* (Figure 2) and promoted glioma apoptosis through excessive autophagy (Figure 3).

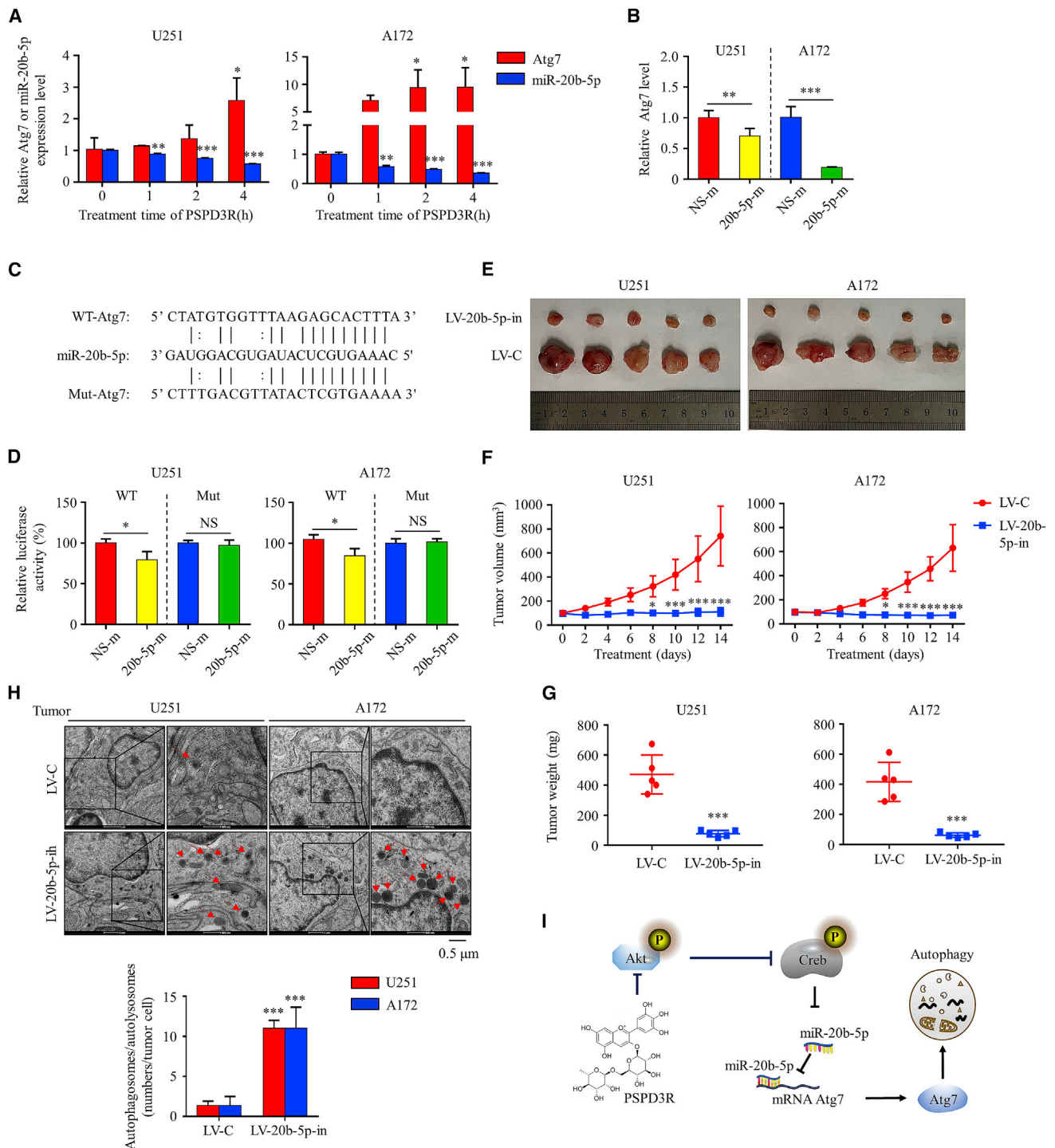


Figure 8. PSPD3R promotes autophagy by regulating miR-20b-5p/Atg7 pathway in glioma cells

(A) The expression of miR-20b-5p and Atg7 mRNA in U251 and A172 cells were measured by quantitative real-time PCR after treatment with the indicated concentrations of PSPD3R within 1, 2, or 4 h (B) U251 and A172 cells were transfected with 20b-5p-m or NS-m, then the expression of Atg7 mRNA was measured by quantitative real-time PCR. (C) The wild-type and mutation of psiCHECK2-Atg7-3'-UTR and its bind sites with miR-20b-5p. (D) U251 and A172 cells were transfected with Atg7-3'-UTR-wild-type or mutant (Mut) plasmid for 6 h and further transfected with 20b-5p-m or NS-m. Luciferase assays were performed, and the luciferase activities were measured at 560 nm by a luciferase reporter gene assay kit. (E-G) U251 and A172 cells were transfected with lentiviral miR-20b-5p inhibition construct (LV-20b-5p-in) or control lentiviral vector

(legend continued on next page)

First, compared with that in the control glioma cells, the number of autophagosomes was higher in the PSPD3R-treated glioma cells as observed under a transmission electron microscope (Figure 3B). Second, AO test revealed abundant acidic vesicles in the PSPD3R-treated glioma cells (Figure 3C). Third, LC3- II conversion was increased in PSPD3R-treated glioma cells, as detected by western blot (Figure 3D). However, the addition of 3-MA reversed the effect of PSPD3R on glioma cells (Figure 3).

PSPD3R also significantly affected the miRNA expression of glioma cells U251 (Figure 4) and regulated autophagy in glioma cells via miR-20b-5p (Figures 5 and 6). Immunoblotting showed that nuclear transcription factor Creb could regulate miR-20b-5p (Figure 7). Finally, data of both luciferase and quantitative real-time PCR assays revealed that Atg7 is the target gene of miR-20b-5p (Figure 8).

This study confirmed that PSPD3R promoted glioma apoptosis by inducing excessive autophagy. Current reports on the biological activities of rutin in China and abroad mainly focus on its anti-inflammatory,³⁴ anti-diabetes,³⁵ antioxidant,³⁶ neuroprotective,¹⁴ and anti-tumor³⁷ activities and the nano preparations of antibacterial and anti-allergy particles from this compound.³⁸ Only two studies showed that rutin can increase the cytotoxicity of chemotherapy drugs by inhibiting autophagy. Professor Ma and colleagues³⁹ found that rutin can attenuate doxorubicin-induced cardiotoxicity by reducing autophagy and apoptosis. Professor Zhang and colleagues⁴⁰ found that rutin can also increase the cytotoxicity of temozolomide in GBM by inhibiting autophagy. However, the present results were contrary to these two reports. Here, PSPD3R promoted glioma apoptosis through excessive autophagy (Figures 1, 2, and 3). According to our literature review, this difference can be attributed to the following reasons. First, autophagy is a double-edged sword that can act as a protective mechanism to maintain normal cell function in physiological conditions.⁴¹ However, excessive autophagy induced by nutritional deficiency, DNA damage, or hypoxia could lead to cell death.⁴² In previous studies, rutin reduced autophagy to increase the toxicity of chemotherapy drugs. In the present work, rutin alone was applied to promote glioma cell apoptosis through excessive autophagy. In addition, the same drug might have different effects on cells in different organs or cell lines. Rutin was applied to treat mouse cardiac tissues in Ma's study³⁹ and was used to treat glioma cells in the current work. Similarly, berberine can play an anti-inflammatory role in liver and an anti-tumor role in the digestive system.⁴³ The autophagy-related signaling pathways are mainly ROS/JNK and Akt/mTOR for glioma cells⁴⁴ and IGF-1/Akt and Akt/mTORC1 signaling pathways for myocardial cells.⁴⁵ Therefore, differences in signaling pathways might also lead to variations in drug functions. Third, different compounds may have varying cancer-suppressing mechanisms. The compound used in Zhang's study is troxerutin, whose main constituents

are flavones. Its molecular formula is $C_{33}H_{42}O_{19}$, and its molecular weight is 742.68. The structure of troxerutin is a double bond between C-2 and C-3. Meanwhile, PSPD3R was extracted and purified from purple sweet potato. Its molecular formula is $C_{30}H_{26}O_{14}$, and its molecular weight is 610.519. The main constituents of PSPD3R are anthocyanidins without a carbonyl group in position 4. In conclusion, the current study provides new treatment ideas for patients with glioma.

For the first time, this study revealed that PSPD3R induced autophagy in glioma cells by regulating the transcription factor Creb. As a transcription factor, Creb is highly expressed in various tumors and involved in tumor proliferation, survival, and metastasis; hence, it was considered an important proto-oncogene.³³ However, the relationship between rutin and Creb in glioma has not been reported. In this work, rutin promoted autophagy through the AKT/Creb signaling pathway in glioma cells. At present, only two relevant reports about Creb in glioma are available. Zheng and colleagues reported that Creb knockdown inhibited the proliferation and migration of U251 glioma cells; however, the signaling pathways involved were not investigated.⁴⁶ Shupeng and colleagues⁴⁷ found that miR-433-3p suppressed cell growth and enhanced chemosensitivity by targeting Creb in human glioma; however, this work focused on the importance of miRNA. Creb is only a target protein of miR-433-3p. In addition, the above two studies failed to discuss the importance of Creb as a transcription factor in glioma-suppressor mechanisms. In the current work, PSPD3R promoted the autophagy of glioma cells by inhibiting the expression of Creb. In turn, Creb overexpression completely reversed the autophagy promoted by PSPD3R (Figure 6). The signaling pathway and downstream target genes involving Creb were also determined. In particular, Creb regulated autophagy via miR-20b-5p in glioma. These conclusions might encourage further research on the relationship between Creb and miRNA and broaden the therapeutic targets in glioma.

In this work, we reported that PSPD3R promoted autophagy by reducing miR-20b-5p in glioma cells (Figures 4, 5, 6, and 7). Natural products from the plants in the "affinal drug and diet" have been used as a part of anti-cancer therapy in glioma.⁴ Rutin, a safe anti-cancer drug without side effects, has been studied in recent years. Most of the reports were related to apoptosis and the autophagy signaling pathway;⁴⁸ however, the molecular mechanism of rutin, especially in miRNA regulation, was poorly investigated. The current work pioneered the discovery of miR-20b-5p function in glioma. Only a few studies reported the function of miR-20b-5p in other cancer types. For example, Qiu and colleagues proved that, in myocardial cells, circular RNA HIPK3 (circHIPK3) regulated the autophagy and apoptosis of hypoxia/reoxygenation-stimulated cardiomyocytes through the miR-20b-5p/Atg7 axis.⁴⁹ Tang and colleagues found

(LV-C), and stable cells were selected by puromycin. Then, 1×10^7 of the stable cells were subcutaneously inoculated in the right upper back of Balb/C nude mice. Mice were sacrificed on day 14, and tumors were excised, photographed, measured, and weighted. (H) The autophagy ultrastructure of tumor xenografts was observed by transmission electron microscope. Red arrows, autophagosomes. Scale bar, 0.5 μ m. (I) Proposed model for the role of PSPD3R in regulating the autophagy in glioma cells. Data are presented as mean \pm SD from three independent experiments. t test for two experimental groups comparisons; *p < 0.05; **p < 0.01; ***p < 0.001.

that long noncoding RNA HOTAIR regulated autophagy through the miR-20b-5p/Atg7 axis in hepatic ischemia/reperfusion injury in the liver.⁵⁰ Study in breast cancer indicated that rutin restrained the growth and metastasis of mouse breast cancer cells by regulating the miRNA-129-1-3p-mediated calcium signaling pathway.⁵¹ Among these three reports about miR-20b-5p, the last two were consistent with the current result, that is, rutin plays an anti-cancer role by regulating miRNA. However, none of the above studies emphasized the function of rutin on regulating miRNA in glioma. The present findings were discovered in glioma cells, in which PSPD3R increased the expression of Atg7 mRNA by downregulating miR-20b-5p to increase autophagy and promote apoptosis (Figure 8). Therefore, the miR-20b-5p/Atg7 axis can be used as a new strategy for the treatment of glioma. Further research might provide a new target gene for the diagnosis and treatment for glioma.

In conclusion, PSPD3R induced the excessive autophagy of glioma cells and led to cell apoptosis by inhibiting AKT phosphorylation, dephosphorylating Creb, downregulating miR-20b-5p, and eventually increasing Atg7 expression and LC3-II conversion.

These results provide novel insights into rutin treatment for glioma. Compared with immunotherapy, PSPD3R is cheaper and easier to obtain, thus relieving the economic pressure on patients. Further investigation on the potential mechanism of PSPD3R in glioma will provide a pharmacologic theoretical basis for its clinical application.

MATERIALS AND METHODS

Mice

Male Balb/c nude mice at 8 weeks of age were purchased from Beijing Charles River Laboratory Animal (Beijing, China) and bred in a special pathogen-free room. All studies were approved by the Institutional Animal Care and Treatment Committee of Xuzhou Medical University. Animal experimental procedures, including treatment, care, and endpoint choice, followed the guidelines of animal research for reporting *in vivo* experiments and were performed with randomization. For the establishment of a subcutaneous glioma model, 1×10^7 U251 or A172 cells were suspended in saline solution and inoculated on the right upper back of each mouse. When the tumor volumes reached approximately 100 mm^3 , the mice were randomized into three groups: one group was injected intraperitoneally with 200 μL of saline solution, and the remaining two groups were administered with 1 or 5 mg/kg PSPD3R every 2 days. All mice were euthanized after 2 weeks for analysis. Tumor tissues were isolated and immediately frozen in liquid nitrogen or fixed in 4% paraformaldehyde (VICMED, Xuzhou, China).

Cell culture

Human glioma cell lines U251, human glioma cell lines A172, mouse normal neuroglial cell line BV2, MH-S murine alveolar macrophages (AMs), mouse lung epithelial cells MLE-12, and HUVECs were obtained from American Type Culture Collection (ATCC, Manassas, VA, USA). All cell lines were cultured in accordance with the ATCC guidelines and used within 6 months. Primary cultures of

rat AST were obtained from neonatal SD rats according to a protocol used previously.⁵² U251, A172, and BV2 cells were maintained in DMEM/high-glucose medium (HyClone, Logan, UT, USA), MLE-12 cells were maintained in DMEM/F-12 medium (HyClone), and MH-S and HUVECs were maintained in RPMI 1640 medium (HyClone). All media were supplemented with 100 U/mL penicillin-streptomycin (Beyotime, Shanghai, China) and 10% serum (Clark Bioscience, Richmond, VA, USA) and placed in a humidified incubator at 37°C under 5% CO₂ atmosphere (Xuzhou Xinhong Special Gas, Xuzhou, China).⁵³

Assays for cell viability

Cell viability was determined by alamar blue (Sigma-Aldrich, St. Louis, MO, USA) assay. The cells were plated at 1×10^4 cells per well of 96-well microtiter plates with 200 μL complete culture medium and treated with indicated PSPD3R concentrations for 12, 24, or 48 h at 37°C in a humidified chamber. Treatment with each PSPD3R concentration was replicated in four wells. After incubation in a humidified incubator for specified times at 37°C, each well was added with alamar blue reagent (200 μL , 0.125 mg/mL in PBS) and incubated for 4 h. Fluorescence intensity was recorded on a microplate reader (Synergy 2; BioTek, Winooski, VT, USA) at 530 nm wavelength. The effect of PSPD3R on growth inhibition was assessed as the inhibition percentage of cell growth, in which vehicle-treated cells were taken as 100% viable. Half maximal inhibitory concentrations (IC50) values were determined from three independent experiments.

Clonogenic assay

The cells were plated at a low density and incubated with increasing PSPD3R concentrations. At the end of the growth period, the cells were fixed with methyl alcohol, stained with Giemsa stain (Solarbio, Beijing, China), and photographed to estimate their proliferation relative to that of untreated cells.⁵⁴

EdU for cellular viability

Cell viability was determined by EdU (RiboBio, Guangzhou, China) assay.²³ The cells were plated at 1×10^4 cells per well in 96-well microtiter plates with 100 μL complete culture medium and treated with designated PSPD3R concentrations (0, 25, 50, and 75 μM) for 24 h at 37°C in a humidified chamber. Treatment with each PSPD3R concentration was replicated in three wells. After incubation, the cells were fixed with 4% paraformaldehyde for 30 min and then exposed to Apollo staining reaction solution. Nuclei were stained with Hoechst33342 Staining Solution, and images were captured using a DM5000 fluorescence microscope (Leica, Buffalo Grove, IL, USA).

Immunohistochemistry

Immunohistochemical analysis was performed as previously described.²³ Tumor tissues from three independent mice were fixed in 4% paraformaldehyde for 2 h and embedded in paraffin following a routine histologic procedure. Tissue blocks were then cut into 4 μm slices, dewaxed, rehydrated, autoclaved for antigen retrieval, blocked with 3% bovine serum albumin (BSA; Beyotime) for 3 h, and finally

incubated with rabbit polyclonal antibodies (Abs) against Ki67 (Proteintech, Wuhan, China) and Alexa Fluor 488-conjugated goat anti-rabbit secondary Ab (Proteintech). Ki67 was detected in tumor tissues using EXPOSE Rabbit Specific HRP/DAB Detection IHC kit (Abcam, Cambridge, UK). Ki67-positive cells were captured under a BX41 microscope (magnification, $\times 400$; Olympus BX43) and counted randomly in six areas per slide.

Flow cytometry

The cells were harvested, washed twice with PBS, and resuspended in Annexin-V FITC/PI solution (KeyGEN, Nanjing, China) for apoptosis analysis. At least 10,000 live cells were analyzed on a flow cytometer (FACS Canto II, BD, Franklin Lakes, NJ, USA). Data were examined with FlowJo software.⁵⁵

Transfection of plasmids, mimic, inhibitors, and LV constructs

miR-20b-5p mimic (20b-5p-m; used for overexpression of miR-20b-5p); NS-m (negative control of 20b-5p-m); 20b-5p-in (used for inhibiting expression of miR-20b-5p); NS-in (negative control of 20b-5p-in); sh-Creb plasmids (used for inhibiting expression of Creb); negative control of shRNA plasmids (sh-NC; negative control of sh-Creb); overexpressed Creb plasmids (oe-Creb; used for overexpression of Creb); empty vector (vector; negative control of oe-Creb); CA-Akt (used for constitutively expression of active Akt); green and red fluorescence protein-tagged LC3 plasmid (LC3-GFP-RFP; used for expression of LC3 with fluorescence); and pcDNA3.1 plasmids (empty vector; negative control of LC3-GFP-RFP) were obtained from Sangon Biotech. LV miR-20b-5p inhibition construct (LV-20b-5p-in; used for inhibiting expression of miR-20b-5p) and LV-C were obtained from Shanghai Genechem (Shanghai, China). U251 and A172 cells were transfected with plasmids or LV constructs using Lipofectamine 3000 (Invitrogen, Carlsbad, CA, USA) or HitransG Transfection Reagent (Genechem, Shanghai, China) in accordance with the manufacturer's instructions.

AO staining

AO staining was performed to evaluate autophagy.⁵⁶ AO (Sigma-Aldrich) was dissolved in PBS containing 5% FBS (10 μM). U251 and A172 cells were treated with or without PSPD3R, 3-MA (Solarbio), miR-20b-5p-m, or oe-Creb plasmid at certain concentrations for 24 h and then incubated with AO at 37°C for 5 min. The cells were then washed three times by PBS and then observed under an Olympus FV10i confocal microscope (FV10-ASW Viewer software). Data were presented as mean \pm SD from three independent experiments.

LC3 puncta observation

U251 and A172 cells were transfected with RFP-GFP tandem fluorescent-tagged LC3 (RFP-GFP-LC3) for 24 h and then treated with 50 μM PSPD3R for another 24 h.⁵⁷ Nuclei were stained with DAPI (Beyotime) to detect the formation of endogenous LC3 puncta in cells using an Olympus FV10i confocal microscope. The obtained images were treated with FV10-ASW Viewer software (scale bar, 10 μm). Data were presented as mean \pm SD from three independent experiments.

Transmission electron microscope observation

First, the cells were treated with PSPD3R or transfected with 20b-5p-in, harvested, fixed in 2.5% glutaraldehyde (Zhongjingkeyi Technology, Kaifeng, China) and 4% paraformaldehyde overnight, added with 1% osmium tetroxide (Zhongjingkeyi Technology), and dehydrated in a series of graded ethanol and acetone (China National Pharmaceutical Group, Beijing, China). The samples were then rinsed and added with 812 epoxy resins (Zhongjingkeyi Technology). Ultrathin sections (70 nm thickness) were prepared using a Leica EM UC7 microtome after polymerization and stained with 3% lead citrate (Zhongjingkeyi Technology) and 2% uranyl acetate (Zhongjingkeyi Technology). Finally, autophagy in cells was observed by a transmission electron microscope (Tecnaï G2 T12; Hillsboro, OR, USA).

Immunoblotting

Rabbit polyclonal Abs against phosphorylated form of Phospho-Creb (#AF3189) were purchased from Affinity Biosciences (Zhenjiang, China). Mouse monoclonal Abs against the total form of Creb (#sc-186) were purchased from Santa Cruz Biotechnology (Santa Cruz, CA, USA). Rabbit polyclonal Abs against the phosphorylated form of Phospho-Akt (#4060) were acquired from Cell Signaling Technology (Danvers, MA, USA). Rabbit polyclonal Abs against LC3 (#14600-1-AP), mouse monoclonal Abs against Atg7 (#67341-1-Ig), and mouse monoclonal Abs against β -actin (#66009-1-Ig) were bought from Proteintech.

The samples derived from cells and tumor homogenates were lysed in whole-cell lysates (KeyGEN), separated by electrophoresis on 10% or 12.5% SDS-polyacrylamide gel electrophoresis, and transferred to nitrocellulose filter membranes (ExCell Bio, Shanghai, China). Proteins were detected using primary Abs at a concentration of 1:1,000 and incubated overnight. Specific interaction with the primary Abs was detected using corresponding secondary Abs conjugated to IR-Dye 800CW Goat (polyclonal) anti-rabbit immunoglobulin G (IgG; H+L) (VICMED) or IRDye 800CW goat (polyclonal) anti-mouse IgG (H+L) (VICMED). Gel bands were observed by the enhanced chemiluminescence Odyssey CLX laser imaging scan system (LICOR, Lincoln, NE, USA) and quantified by ImageJ software. Data were presented as means \pm SD from three independent immunoblotting assays.⁵⁸ Phosphorylated and total protein levels were determined and quantified by three successive immunoblotting experiments.

Quantitative real-time PCR

After treatment, total RNAs were isolated from cells using the Trizol reagent (Vicmed) in accordance with the manufacturer's protocol. RNA concentration was measured using the enzyme standard instrument (Spectrophotometer OD-1000 nanodrop; OneDrop, Shanghai, China). For RNA measurement, cDNA was synthesized using FastKing cDNA reagent kit (TIANGEN, Beijing, China) and miRcute plus miRNA first-strand cDNA kit (TIANGEN) and analyzed by SYBR green methods with SuperReal PreMix Plus (SYBR Green) (TIANGEN) and miRcute plus miRNA qPCR kit (TIANGEN). The program was as follows: 95°C for 15 min, followed by 40 cycles of

95°C for 10 s and 60°C for 20 s. The following primer sequences were used:

Atg7: 5'-GAGCAAGCCCGCAGAGATGTG-3' (forward),

5'-TCCCAAAGCAGCATTGATGACCAG-3' (reverse);

has-miR6132: 5'-CAGCAGGGCTGGGGATTGCA-3' (forward);

has-miR4492: 5'-TATATAGGGGCTGGGCGCGCG-3' (forward);

has-miR-20b-5p: 5'-CGCGCAAAGTGCTCATAGTGCAGGTAG-3' (forward);

has-miR-338-5p: 5'-CGCGCAACAATATCCTGGTGCTGAGTG-3' (forward);

has-miR-3911: 5'-CCTGTGTGGATCCTGGAGGAGGCA-3' (forward);

has-miR-503-5p: 5'-CGTAGCAGCGGGAACAGTTCTGCAG-3' (forward).

The expression of target transcript was calculated by $2^{-\Delta\Delta CT}$ method.⁵⁹ GAPDH and U6 were used as the loading control for mRNA and miRNA, respectively.

Luciferase reporter assays

Wild-type (WT) psiCHECK2-Atg7-3' UTR reporter plasmid and psiCHECK2-Atg7-3' UTR reporter plasmid with a Mut at the miR-20b-5p binding site were purchased from Guangzhou Genesee Biotech. The reporters and miR-20b-5p-m were cotransfected into U251 and A172 cells using Lipofectamine 3000. The cells were harvested and lysed after 24 h of transfection. Luciferase intensity was then measured with Dual-Lumi Luciferase Reporter Gene Assay kit (Beyotime) in accordance with the manufacturer's instructions.⁶⁰

miRNA microarray analysis

U251 cells were plated in 6-well microtiter plates and treated with or without PSPD3R. The total RNA was then extracted using Trizol reagent (VICMED) following the manufacturers' guidelines. miRNA isolation and high-throughput miRNA profiling were performed by CapitalBio Technology (Beijing, China). Microarray data were analyzed using Affymetrix GeneChip Command Console software. The significantly differentially expressed miRNAs between control and PSPD3R-treated groups were selected using ANOVA and a two-tailed t test according to the following criteria: fold change >2 or ≤2 and p <0.05.⁶¹

Statistical analysis

Experiments were performed in triplicate and independently repeated at least three times. Statistical analysis was carried out using GraphPad Prism 7 software. Data are shown as mean ± SD. Statistical differences were evaluated by one-way ANOVA (Tukey's post hoc test) for multiple comparisons or by two-tailed Student's t test for

two experimental group comparisons. Differences were accepted as significant at p <0.05.

Data availability

The data of this research are available from the corresponding author upon request.

SUPPLEMENTAL INFORMATION

Supplemental information can be found online at <https://doi.org/10.1016/j.omto.2022.07.007>.

ACKNOWLEDGMENTS

This research was funded by the National Natural Science Foundation of China (31770613 and 81870005); the Project of Xuzhou Applied and Basic Research (KC21194); the Postgraduate Research & Practice Innovation Program of Jiangsu Province (KYCX20_2080); and the Opening Project of Zhejiang Provincial Preponderant and Characteristic Subject of Key University (Traditional Chinese Pharmacology), Zhejiang Chinese Medical University (ZYAOX2018004). The experiments in this article were partly completed in Public Experimental Research Center and Laboratory Animal Center of Xuzhou Medical University. We sincerely thank all teachers for their enthusiastic help.

AUTHOR CONTRIBUTIONS

J.J. and R.L. conceived and designed the research. M.W. and K.L. performed most of the experiments. H.B., H.C., G.D., N.X., C.L., Y.Z., F.J., and Y.Z. performed the data analyses. B.Y. isolated and purified PSPD3R. M.W. and R.L. wrote the manuscript. R.L. and J.J. reviewed and revised the manuscript.

DECLARATION OF INTERESTS

The authors have no financial conflicts of interest.

REFERENCES

1. McCutcheon, L.E., and Preul, M.C. (2021). Historical perspective on surgery and survival with glioblastoma: how far have we come? *World Neurosurg.* *149*, 148–168.
2. Park, J.H., de Lomana, A.L.G., Marzese, D.M., Juarez, T., Feroze, A., Hothi, P., Cobbs, C., Patel, A.P., Kesari, S., Huang, S., and Baliga, N.S. (2021). A systems approach to brain tumor treatment. *Cancers* *13*, 3152.
3. Lu, V.M., Jue, T.R., McDonald, K.L., and Rovin, R.A. (2018). The survival effect of repeat surgery at glioblastoma recurrence and its trend: a systematic review and meta-analysis. *World Neurosurg.* *115*, 453–459.e3.
4. Erices, J.I., Torres, Á., Niechi, I., Bernales, I., and Quezada, C. (2018). Current natural therapies in the treatment against glioblastoma. *Phytother. Res.* *32*, 2191–2201.
5. Chen, T., Yang, Y., Zhu, S., Lu, Y., Zhu, L., Wang, Y., and Wang, X. (2020). Inhibition of Aβ aggregates in Alzheimer's disease by epigallocatechin and epicatechin-3-gallate from green tea. *Bioorg. Chem.* *105*, 104382.
6. Yang, T., Zang, D.W., Shan, W., Guo, A.C., Wu, J.P., Wang, Y.J., and Wang, Q. (2019). Synthesis and evaluations of novel apocynin derivatives as anti-hlioma agents. *Front. Pharmacol.* *10*, 951.
7. Luthra, P.M., and Lal, N. (2016). Prospective of curcumin, a pleiotropic signalling molecule from *Curcuma longa* in the treatment of glioblastoma. *Eur. J. Med. Chem.* *109*, 23–35.
8. Kiskova, T., Kubatka, P., Büsselberg, D., and Kassayova, M. (2020). The plant-derived compound resveratrol in brain cancer: a review. *Biomolecules* *10*, 161.

9. Lee, J.E., Yoon, S.S., and Moon, E.Y. (2019). Curcumin-induced autophagy augments its antitumor effect against A172 human glioblastoma cells. *Biomol. Ther.* 27, 484–491.
10. Ono, K., Zhao, D., Wu, Q., Simon, J., Wang, J., Radu, A., and Pasinetti, G.M. (2020). Pine bark polyphenolic extract attenuates amyloid- β and Tau misfolding in a model system of Alzheimer's disease neuropathology. *J. Alzheimers Dis.* 73, 1597–1606.
11. Jain, K.K. (2018). A critical overview of targeted therapies for glioblastoma. *Front. Oncol.* 8, 419.
12. Xiao, J., Capanoglu, E., Jassbi, A.R., and Miron, A. (2016). Advance on the flavonoid C-glycosides and health benefits. *Crit. Rev. Food Sci. Nutr.* 56, S29–S45.
13. Abotaleb, M., Samuel, S., Varghese, E., Varghese, S., Kubatka, P., Liskova, A., and Büsselberg, D. (2018). Flavonoids in cancer and apoptosis. *Cancers (Basel)*. 11, 28.
14. Enogieru, A.B., Haylett, W., Hiss, D.C., Bardien, S., and Ekpo, O.E. (2018). Rutin as a potent antioxidant: implications for neurodegenerative disorders. *Oxidative Med. Cell Longevity* 2018, 6241017.
15. Fan, S., Yang, G., Zhang, J., Li, J., and Bai, B. (2020). Optimization of ultrasound-assisted extraction using response surface methodology for simultaneous quantitation of six flavonoids in *Flos Sophorae Immaturus* and antioxidant activity. *Molecules* 25, 1767.
16. Liew, S.S., Ho, W.Y., Yeap, S.K., and Sharifudin, S.A.B. (2018). Phytochemical composition and in vitro antioxidant activities of *Citrus sinensis* peel extracts. *PeerJ* 6, e5331.
17. Tang, G.Y., Zhao, C.N., Liu, Q., Feng, X.L., Xu, X.Y., Cao, S.Y., Meng, X., Li, S., Gan, R.Y., and Li, H.B. (2018). Potential of grape wastes as a natural source of bioactive compounds. *Molecules* 23, 2598.
18. da Silva, A.B., Cerqueira Coelho, P.L., das Neves Oliveira, M., Oliveira, J.L., Oliveira Amparo, J.A., da Silva, K.C., Soares, J.R.P., Pitanga, B.P.S., Dos Santos Souza, C., de Faria Lopes, G.P., et al. (2020). The flavonoid rutin and its aglycone quercetin modulate the microglia inflammatory profile improving antiangioma activity. *Brain Behav. Immun.* 85, 170–185.
19. de Oliveira, C.T.P., Colenci, R., Pacheco, C.C., Mariano, P.M., do Prado, P.R., Mamprin, G.P.R., Santana, M.G., Gambero, A., de Oliveira Carvalho, P., and Prioli, D.G. (2019). Hydrolyzed rutin decreases worsening of anaplasia in glioblastoma relapse. *CNS Neurol. Disord. Drug Targets* 18, 405–412.
20. Wang, H., Fan, W., Li, H., Yang, J., Huang, J., and Zhang, P. (2013). Functional characterization of Dihydroflavonol-4-reductase in anthocyanin biosynthesis of purple sweet potato underlies the direct evidence of anthocyanins function against abiotic stresses. *PLoS One* 8, e78484.
21. Dong, G., Xu, N., Wang, M., Zhao, Y., Jiang, F., Bu, H., Liu, J., Yuan, B., and Li, R. (2021). Anthocyanin extract from purple sweet potato exacerbate mitophagy to ameliorate pyroptosis in *Klebsiella pneumoniae* infection. *Int. J. Mol. Sci.* 22, 11422.
22. Mu, M., Niu, W., Zhang, X., Hu, S., and Niu, C. (2020). LncRNA BCYRN1 inhibits glioma tumorigenesis by competitively binding with miR-619-5p to regulate CUEDC2 expression and the PTEN/AKT/p21 pathway. *Oncogene* 39, 6879–6892.
23. Bu, H., Tan, S., Yuan, B., Huang, X., Jiang, J., Wu, Y., Jiang, J., and Li, R. (2021). Therapeutic potential of IBP as an autophagy inducer for treating lung cancer via blocking PAK1/Akt/mTOR signaling. *Mol. Ther. Oncolytics* 20, 82–93.
24. Zhou, M., Zhang, G., Hu, J., Zhu, Y., Lan, H., Shen, X., Lv, Y., and Huang, L. (2021). Rutin attenuates Sorafenib-induced chemoresistance and autophagy in hepatocellular carcinoma by regulating BANCER/miRNA-590-5P/OLR1 axis. *Int. J. Biol. Sci.* 17, 3595–3607.
25. Ai, X., Ye, Z., Yao, Y., Xiao, J., You, C., Xu, J., Huang, X., Zhong, J., Fan, M., Song, X., et al. (2020). Endothelial autophagy: an effective target for radiation-induced cerebral capillary damage. *Sci. Rep.* 10, 614.
26. Escamilla-Ramírez, A., Castillo-Rodríguez, R.A., Zavala-Vega, S., Jimenez-Farfan, D., Anaya-Rubio, I., Briseño, E., Palencia, G., Guevara, P., Cruz-Salgado, A., Sotelo, J., and Trejo-Solís, C. (2020). Autophagy as a potential therapy for malignant glioma. *Pharmaceuticals (Basel)*. 13, 156.
27. Thomé, M.P., Filippi-Chiela, E.C., Villodre, E.S., Migliavaca, C.B., Onzi, G.R., Felipe, K.B., and Lenz, G. (2016). Ratiometric analysis of acridine orange staining in the study of acidic organelles and autophagy. *J. Cell Sci.* 129, 4622–4632.
28. Mansoori, B., Mohammadi, A., Shirjang, S., and Baradaran, B. (2017). MicroRNAs in the diagnosis and treatment of cancer. *Immunol. Invest.* 46, 880–897.
29. Revathidevi, S., and Munirajan, A.K. (2019). Akt in cancer: mediator and more. *Semin. Cancer Biol.* 59, 80–91.
30. Zhang, Q., Wang, X., Cao, S., Sun, Y., He, X., Jiang, B., Yu, Y., Duan, J., Qiu, F., and Kang, N. (2020). Berberine represses human gastric cancer cell growth in vitro and in vivo by inducing cytostatic autophagy via inhibition of MAPK/mTOR/p70S6K and Akt signaling pathways. *Biomed. Pharmacother.* 128, 110245.
31. Xu, Z., Han, X., Ou, D., Liu, T., Li, Z., Jiang, G., Liu, J., and Zhang, J. (2020). Targeting PI3K/AKT/mTOR-mediated autophagy for tumor therapy. *Appl. Microbiol. Biotechnol.* 104, 575–587.
32. Ma, Y., Dong, C., Chen, X., Zhu, R., and Wang, J. (2021). Silencing of miR-20b-5p exerts inhibitory effect on diabetic retinopathy via inactivation of THBS1 gene induced VEGF/Akt/PI3K Pathway. *Diabetes Metab. Syndr. Obes.* 14, 1183–1193.
33. Sapio, L., Salzillo, A., Ragone, A., Illiano, M., Spina, A., and Naviglio, S. (2020). Targeting CREB in cancer therapy: a key candidate or one of many? An update. *Cancers (Basel)*. 12, 3166.
34. Yi, Y.S. (2018). Regulatory roles of flavonoids on inflammasome activation during inflammatory responses. *Mol. Nutr. Food Res.* 62, e1800147.
35. Ghorbani, A. (2017). Mechanisms of antidiabetic effects of flavonoid rutin. *Biomed. Pharmacother.* 96, 305–312.
36. Arowoogun, J., Akanni, O.O., Adefisan, A.O., Owumi, S.E., Tijani, A.S., and Adaramoye, O.A. (2021). Rutin ameliorates copper sulfate-induced brain damage via antioxidative and anti-inflammatory activities in rats. *J. Biochem. Mol. Toxicol.* 35, e22623.
37. Imani, A., Maleki, N., Bohlouli, S., Kouhsoltani, M., Sharifi, S., and Maleki Dizaj, S. (2021). Molecular mechanisms of anticancer effect of rutin. *Phytotherapy Res.* 35, 2500–2513.
38. Negahdari, R., Bohlouli, S., Sharifi, S., Maleki Dizaj, S., Rahbar Saadat, Y., Khezri, K., Jafari, S., Ahmadian, E., Gorbani Jahandizi, N., and Raeesi, S. (2021). Therapeutic benefits of rutin and its nanoformulations. *Phytother. Res.* 35, 1719–1738.
39. Ma, Y., Yang, L., Ma, J., Lu, L., Wang, X., Ren, J., and Yang, J. (2017). Rutin attenuates doxorubicin-induced cardiotoxicity via regulating autophagy and apoptosis. *Biochim. Biophys. Acta Mol. Basis Dis.* 1863, 1904–1911.
40. Zhang, P., Sun, S., Li, N., Ho, A.S.W., Kiang, K.M.Y., Zhang, X., Cheng, Y.S., Poon, M.W., Lee, D., Pu, J.K.S., and Leung, G.K.K. (2017). Rutin increases the cytotoxicity of temozolomide in glioblastoma via autophagy inhibition. *J. Neurooncol.* 132, 393–400.
41. Kim, S.H., Kim, K.Y., Park, S.G., Yu, S.N., Kim, Y.W., Nam, H.W., An, H.H., Kim, Y.W., and Ahn, S.C. (2017). Mitochondrial ROS activates ERK/autophagy pathway as a protected mechanism against deoxyribose-induced apoptosis. *Oncotarget* 8, 111581–111596.
42. Bhattacharya, A., and Eissa, N.T. (2015). Autophagy as a stress response pathway in the immune system. *Int. Rev. Immunol.* 34, 382–402.
43. Zou, K., Li, Z., Zhang, Y., Zhang, H.Y., Li, B., Zhu, W.L., Shi, J.Y., Jia, Q., and Li, Y.M. (2017). Advances in the study of berberine and its derivatives: a focus on anti-inflammatory and anti-tumor effects in the digestive system. *Acta Pharmacol. Sin.* 38, 157–167.
44. Liu, X., Zhao, P., Wang, X., Wang, L., Zhu, Y., Song, Y., and Gao, W. (2019). Celastrol mediates autophagy and apoptosis via the ROS/JNK and Akt/mTOR signaling pathways in glioma cells. *J. Exp. Clin. Cancer Res.* 38, 184.
45. Miyamoto, S. (2019). Autophagy and cardiac aging. *Cell Death Differ.* 26, 653–664.
46. Zheng, K.B., Xie, J., Li, Y.T., Yuan, Y., Wang, Y., Li, C., and Shi, Y.F. (2019). Knockdown of CERB expression inhibits proliferation and migration of glioma cells line U251. (2019). *Bratisl. Lek. Listy* 120, 309–315.
47. Sun, S., Wang, X., Xu, X., Di, H., Du, J., Xu, B., Wang, Q., and Wang, J. (2017). MiR-433-3p suppresses cell growth and enhances chemosensitivity by targeting CREB in human glioma. *Oncotarget* 8, 5057–5068.
48. Nouri, Z., Fakhri, S., Nouri, K., Wallace, C.E., Farzaei, M.H., and Bishayee, A. (2020). Targeting multiple signaling pathways in cancer: the rutin therapeutic approach. *Cancers* 12, 2276.

49. Qiu, Z., Wang, Y., Liu, W., Li, C., Zhao, R., Long, X., Rong, J., Deng, W., Shen, C., Yuan, J., et al. (2021). CircHIPK3 regulates the autophagy and apoptosis of hypoxia/reoxygenation-stimulated cardiomyocytes via the miR-20b-5p/ATG7 axis. *Cell Death Discov.* *7*, 64.
50. Tang, B., Bao, N., He, G., and Wang, J. (2019). Long noncoding RNA HOTAIR regulates autophagy via the miR-20b-5p/ATG7 axis in hepatic ischemia/reperfusion injury. *Gene* *686*, 56–62.
51. Li, Q., Xu, D., Gu, Z., Li, T., Huang, P., and Ren, L. (2021). Rutin restrains the growth and metastasis of mouse breast cancer cells by regulating the microRNA-129-1-3p-mediated calcium signaling pathway. *J. Biochem. Mol. Toxicol.* *35*, e22794.
52. Su, H., Fan, S., Zhang, L., and Qi, H. (2021). TMAO aggregates neurological damage following ischemic stroke by promoting reactive astrocytosis and glial scar formation via the Smurf2/ALK5 axis. *Front. Cell. Neurosci.* *15*, 569424.
53. Li, W., Du, Q., Li, X., Zheng, X., Lv, F., Xi, X., Huang, G., Yang, J., and Liu, S. (2020). Eriodictyol inhibits proliferation, metastasis and induces apoptosis of glioma cells via PI3K/Akt/NF- κ B signaling pathway. *Front. Pharmacol.* *11*, 114.
54. Valable, S., G erault, A.N., Lambert, G., Leblond, M.M., Anfray, C., Toutain, J., Bordji, K., Petit, E., Bernaudin, M., and P er s, E.A. (2020). Impact of hypoxia on carbon ion therapy in glioblastoma cells: modulation by LET and hypoxia-dependent Genes. *Cancers* *12*, 2019.
55. Yang, Q., Deng, L., Li, J., Miao, P., Liu, W., and Huang, Q. (2020). NR5A2 promotes cell growth and resistance to temozolomide through regulating Notch signal pathway in glioma. *Onco. Targets Ther.* *13*, 10231–10244.
56. Hseu, Y.C., Lin, R.W., Shen, Y.C., Lin, K.Y., Liao, J.W., Thiagarajan, V., and Yang, H.L. (2020). Flavokawain B and doxorubicin work synergistically to impede the propagation of gastric cancer cells via ROS-mediated apoptosis and autophagy pathways. *Cancers* *12*, 2475.
57. Xiao, Q., Liu, H., Wang, H.S., Cao, M.T., Meng, X.J., Xiang, Y.L., Zhang, Y.Q., Shu, F., Zhang, Q.G., Shan, H., and Jiang, G.M. (2020). Histone deacetylase inhibitors promote epithelial-mesenchymal transition in Hepatocellular Carcinoma via AMPK-FOXO1-ULK1 signaling axis-mediated autophagy. *Theranostics* *10*, 10245–10261.
58. Wang, M., Li, F., Shi, Z., Liu, Y., Wang, X., Li, L., and Gao, D. (2014). N-cadherin is a novel ER α anchor that protects against 6-OHDA damage to dopaminergic cells. *Cell. Mol. Neurobiol.* *34*, 123–131.
59. He, X., Chai, P., Li, F., Zhang, L., Zhou, C., Yuan, X., Li, Y., Yang, J., Luo, Y., Ge, S., et al. (2020). A novel LncRNA transcript, RBAT1, accelerates tumorigenesis through interacting with HNRNPL and cis-activating E₂F₃. *Mol. Cancer* *19*, 115.
60. Cheng, W., Wang, K., Zhao, Z., Mao, Q., Wang, G., Li, Q., Fu, Z., Jiang, Z., Wang, J., and Li, J. (2020). Exosomes-mediated transfer of miR-125a/b in cell-to-cell communication: a novel mechanism of genetic exchange in the intestinal microenvironment. *Theranostics* *10*, 7561–7580.
61. Chen, S., Lao, J., Geng, Q., Zhang, J., Wu, A., and Xu, D. (2020). A 3-microRNA signature identified from serum predicts clinical outcome of the locally advanced gastric cancer. *Front. Oncol.* *10*, 565.